



# Finite element analysis comparing short-segment instrumentation with conventional pedicle screws and the Schanz pedicle screw in lumbar 1 fractures

Fei Zhou<sup>1</sup> · Sheng Yang<sup>1</sup> · Jifeng Liu<sup>1</sup> · Jianmin Lu<sup>1</sup> · Depeng Shang<sup>1</sup> · Chao Chen<sup>1</sup> · Huanhuan Wang<sup>1</sup> · Jinming Ma<sup>1</sup>

Received: 27 March 2019 / Revised: 10 July 2019 / Accepted: 16 July 2019 / Published online: 2 August 2019  
© Springer-Verlag GmbH Germany, part of Springer Nature 2019

## Abstract

Previous finite element studies of thoracolumbar fractures were mostly based on simulation analysis of one single object, which was difficult to objectively evaluate the differences between conventional pedicle screws and Schanz pedicle screws. The aim of this study was to evaluate the stress of screw and injured vertebrae displacement using the finite element model of conventional pedicle screw and Schanz pedicle screw instrumentation for the treatment of lumbar 1 fractures. Data of eight healthy volunteers were used to simulate the finite element model. The instrumentation models were divided into four groups: moderate fracture conventional (MC), moderate fracture Schanz (MS), unstable/severe fracture conventional (UC), and unstable/severe fracture Schanz (US) pedicle screw groups. The maximum screw stress and lumbar 1 displacement/micro-motion in each group increased with the increase of torque and/or load. Under the same fracture, maximum von Mises stress of conventional pedicle screw (MC/UC) was larger than Schanz pedicle screw (MS/US) ( $P < 0.05$ ) and lumbar 1 displacement/micro-motion of Schanz pedicle screw (MS/US) was larger than conventional pedicle screw (MC/UC) ( $P < 0.05$ ). Under the same screws, the maximum von Mises stress and displacement/micro-motion of unstable fracture (UC/US) were larger than moderate fracture (MC/MS) ( $P < 0.05$ ). Posterior short-segment instrumentation with Schanz pedicle screws were recommended for unstable fractures. The compression displacement/micro-motion of bony defect during flexion may lead to the postoperative re-collapse of injured vertebrae.

**Keywords** Lumbar 1 fractures · Pedicle screw instrumentation · Stress · Displacement/micro-motion of bony defect · Finite element

## Background

Thoracolumbar fractures are the most common spinal injuries, and surgery is required for severe fractures [1, 2]. Conventional

pedicle screw instrumentation has been widely used due to its advantages of small trauma, less bleeding, and less interference with adjacent segments [3, 4]. However, complications such as breakage and/or loosening of the screw after instrumentation,

Fei Zhou, Sheng Yang, and Jifeng Liu equally contributed to this paper and thus shared the co-first authorship.

✉ Sheng Yang  
yangsheng\_88@163.com

Fei Zhou  
zhoufei20180110@163.com

Jifeng Liu  
377714406@qq.com

Jianmin Lu  
jianminlu369@sina.com

Depeng Shang  
499645354@qq.com

Chao Chen  
1957261399@qq.com

Huanhuan Wang  
1697849282@qq.com

Jinming Ma  
1542500945@qq.com

<sup>1</sup> Department of Orthopaedics, Affiliated Zhongshan Hospital of Dalian University, No. 6 Jiefang Street, Zhongshan District, Dalian 116001, Liaoning, China

re-collapse of the injured vertebrae, and kyphosis recurrence for unstable/severe fractures (load-sharing classification (LSC) [5]  $\geq 7$ ) restrict the application of this method [6]. To avoid these complications, the addition of 2 screws inserted in the fractured vertebra (6-screw construct) and/or augmentation for the severe fractures have been introduced [7]. However, screw breakage remains unavoidable [8, 9].

Different from the abovementioned auxiliary treatment methods, we [10] and Aono et al. [1] achieved good results using posterior short-segment instrumentation with Schanz pedicle screw (1 level above and 1 level below the fractured vertebra) to treat unstable thoracolumbar spine fractures without complications such as breakage or loosening of screws. In our previous study [10], we firstly speculated that the Schanz pedicle screw is superior to conventional pedicle screw due to the structure and load transmission of the Schanz screw rod (similar to “J”-shaped conduction) which are more similar to the lumbar posterior column (butterfly-shaped conduction) than conventional pedicle screw (similar to “|”-shaped conduction).

Despite the fact that Schanz pedicle screw has been effective in treating unstable fractures, it still has the disadvantages of postoperative re-collapse of the injured vertebra, tedious operation, and more damage to paravertebral soft tissue than conventional screws, which hindered its extensive application [11]. Jang et al. retrospectively analyzed the re-collapsed 31 of 208 cases after posterior instrumented fusion in thoracolumbar burst fracture and stated that age ( $> 43$  years) and preoperative body height loss ( $> 54\%$ ) were the risk factors for body re-collapse [11]. However, we believe that displacement/micro-motion of the bony defect is the main cause of re-collapse since re-collapse was avoided after the Schanz pedicle screw instrumentation combined with thoracolumbosacral orthosis (TLSO) brace in our previous article [10]. TLSO brace can limit the thoracolumbar sacral movement to reduce the injured vertebrae displacement/micro-motion and thus avoid the re-collapse of the injured vertebrae [10]. Therefore, we hope to verify the advantages of the Schanz pedicle screw and the cause of the re-collapse of the injured vertebra by this study.

In this study, we first established a bony defect model based on LSC. Using a finite element method, the authors firstly analyzed and compared the screw stress and bony defect displacement/micro-motion after the short-segment instrumentation with conventional and Schanz pedicle screws for the moderate and unstable fractures. From the perspective of biomechanics, we hope to find the evidence to support our speculation mentioned above.

## Methods

A total of 8 (7 males and 1 female) healthy young subjects participated in the experiment, aged  $26.75 \pm 2.55$  years old, with height of  $174.63 \pm 5.26$  cm and body weight of  $74.88 \pm$

$7.86$  kg. This study was approved by the Ethics Committee of Affiliated Zhongshan Hospital of Dalian University. All participants provided written informed consent.

## The finite element model

### Normal T12-L2 model

DICOM format files of 8 subjects were obtained by continuously scanning with a 64-slice spiral computed tomography (CT). The slice thickness was 0.75 mm. The finite element model was created using software including MIMICS 17.0 (Materialise Inc., Leuven, Belgium), Geomagic studio 2013 (Geomagic, Inc., Research Triangle Park, NC, USA), and Hypermesh 13.0 (Altair Engineering, Inc., Executive Park, CA, USA). Firstly, the CT data in DICOM format were exported to MIMICS to obtain a multilayer continuous image of the coronal, sagittal, and horizontal positions, and the appropriate gray value was set to 275 to highlight the bone structure. The three vertebrae of the T12-L2 segment were subjected to Thresholding, Region Growing, Edit Masks, and Calculate 3D to reconstruct the preliminary three-dimensional geometric model. Subsequently, the model was then imported into Geomagic studio software in STL format. Grid doctor was used to smooth the surface of the model, repair the holes, and remove the spikes. The model was then fitted to an accurate NURBS surface using the probabilistic curvature method at the exact surface stage. Finally, the NURBS surface was imported into the Hypermesh software in Iges format for meshing, and the corresponding structures were established including the vertebral body, intervertebral disc, and paraspinal ligament. The vertebral body is composed of the cortical bone, cancellous bone, and endplate, and the thickness of the cortical bone and endplate is set to 1 mm. The intervertebral disc consisted of nucleus pulposus (NP) and annulus fibrosus. The volume ratio of the annulus fibrosus to NP was set to 7:3. The vertebral body is bound to the adjacent intervertebral disc. The thickness of the articular cartilage was set to 0.3 mm, and the upper and lower articular cartilages were in frictional contact with a friction coefficient of 0.1. Seven paravertebral ligaments were simulated including the anterior longitudinal ligament, posterior longitudinal ligament, ligamentum flavum, interspinous ligament, supraspinous ligament, capsular ligament, and intertransverse ligament. These model materials and properties were selected according to the previous studies [12, 13]. The final intact T12-L2 model includes  $98,477 \pm 17,964$  elements and  $28,567 \pm 3737$  nodes.

### Internal fixation model

According to previous reports by Kubosch et al. [14] and Liao et al. [15], the diameter of conventional pedicle screw and connecting rod in this study was set to 6.5 mm and 6 mm,

respectively, and the width and height of the transverse rod connector were 3 mm and 4 mm, respectively. The diameter of Schanz pedicle screw and connecting rod was set to 6.2 mm and 6 mm, respectively. The screw placement was performed using a Roy-Camille method, and screws were inserted paralleled to the superior endplate with a placement depth of 80% according to our previous article [10].

The methods reported by Liu et al. [12] were used to simulate the type A L1 fracture [16] through the equivalent removal of the anterior and middle columns of the L1 vertebrae. As for the bony defect area, the front side is the anterior margin of the vertebral body, the upper side is a transection paralleled to the upper endplate, and the lower side is an oblique section paralleled to the kyphotic correction angle [5]. The size of the bony defect varied with the fracture severity (Fig. 1). The ratio of AUVH (anterior upper vertebral body (UB) height above the bony defect) is equal to  $AUVH/AVH$  (anterior vertebral body height)  $\times 100\%$ ; the ratio of ALVH (anterior lower vertebral body height below the bony defect) is equal to  $ALVH/AVH \times 100\%$ ; the ratio of anterior bony defect height (ADH) is equal to  $ADH/AVH \times 100\%$ . For moderate fractures (LSC 5–6 points, MF), the AVH compression was set to 45% of the original height before fracture reduction. After reduction, the ratio of AUVH, ratio of ADH, and ratio of ALVH were 15%, 30%, and 55% respectively. The kyphotic correction angle was  $6^\circ$  and the posterior wall of the vertebral body was continuous. For unstable/severe fractures (LSC  $\geq 7$  points, UF), the AVH compression was set to 65% of the original height before fracture reduction. After reduction, AUVH, ADH, and ALVH accounted for 15%, 50%, and 35% respectively. The kyphotic correction angle was  $12^\circ$  [5]. Four instrumentation models were established: moderate fracture conventional (MC) pedicle screw group, moderate fracture Schanz (MS) pedicle screw group, unstable fracture conventional (UC) pedicle screw group, and unstable fracture Schanz (US) pedicle screw group. MC group consisted of  $225,641 \pm 21,829$  elements and  $51,341 \pm 4691$  nodes. The MS group consisted of  $211,547 \pm 21,781$  elements and  $48,059 \pm 4668$  nodes. The UC group contains  $223,658 \pm 21,518$  elements and  $50,975 \pm 4643$  nodes. The US group contains  $209,548 \pm 21,499$  elements and  $47,691 \pm 4622$  nodes.

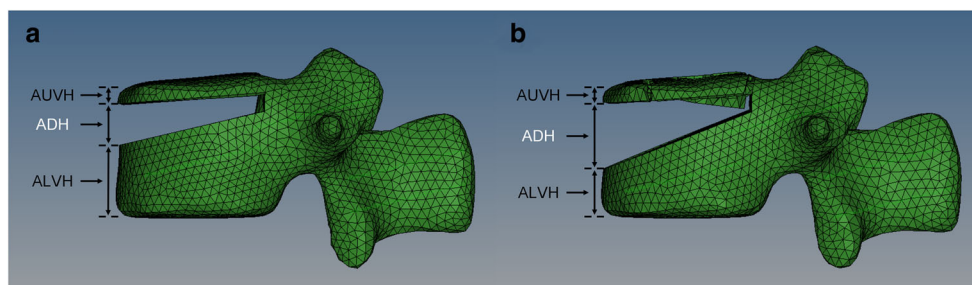


**Fig. 1** Lateral projection of L1 fracture after reduction. **a** After reduction of moderate fractures, ratio of the anterior upper vertebral body height above the bony defect (AUVH), ratio of the anterior bony defect (ADH), and ratio of the anterior lower vertebral body height below the bony

## Finite element analysis

The lower surface of the L2 vertebral body was constrained and completely fixed. The junction of the screw and the bone is a continuous mesh and sharing node. According to previous studies [17–22], the following loads were applied to the upper surface of the T12 vertebral body, respectively, and finite element software (Abaqus CAE 6.13) was used to analyze the screw stress and the displacement/micro-motion of L1 vertebra of each group.

- (1) Pure torque during anterior flexion: 5 Nm, 10 Nm, 15 Nm;
- (2) Vertical loads: 150 N, 350 N, 500 N;
- (3) Torque of 10 Nm during flexion/extension, lateral bending, rotation, and vertical load of 350 N.

## Statistical analysis

Statistical analyses were performed using SPSS 20.0 (SPSS Inc., Chicago, IL, USA). Data were expressed as mean  $\pm$  standard deviation (SD). A paired sample *t* test was used to compare the conventional pedicle screw and the Schanz pedicle screw, and an independent sample *t* test was used to compare the moderate and severe fractures. A two-sided *P* value of less than 0.05 was considered statistically significant.

## Result

### Validation of the model

In this study, the kyphotic angle of the eight T12-L2 segment models was  $9.8 \pm 5.6^\circ$ , and the total height of the T12-L2 vertebral body leading edge (including T12-L1 and L1-2 intervertebral discs) was  $92.2 \pm 5.1$  mm. The range of motion (ROM) of T12/L1 and L1/L2 vertebra of the normal T12-L2 model was similar to those of Panjabi et al. [23] and

defect (ALVH) were 15%, 30%, and 55% respectively. The kyphotic correction angle was  $6^\circ$ . **b** After reduction of unstable fractures, AUVH, ADH, and ALVH accounted for 15%, 50%, and 35% respectively. The kyphotic correction angle was  $12^\circ$

Yamamoto et al. [24] (Fig. 2). Therefore, the T12-L2 model in this study was valid for further analyses.

### Pedicle screw stress

The length of conventional pedicle screw and Schanz pedicle screw was  $46.7 \pm 3.2$  mm and  $47.0 \pm 3.7$  mm, respectively ( $P > 0.05$ ). The fatigue threshold of the pedicle screw was 550 MPa, the yielding threshold was 869 MPa, and the breakage threshold was 924 MPa according to a previous study [25].

### Pure torque, pure vertical loads, or torque plus different vertical loads during anterior flexion

When flexion torque, vertical load, or flexion torque plus vertical load was applied, the maximum von Mises stress of the upper and lower screws in each group increased with the increase of torque or load, and the maximum von Mises stress was concentrated at the root of the upper screws. The maximum von Mises stress of the lower screws in each group is lower than the fatigue threshold of 550 MPa (Tables 1 and 2). The stress nephogram of the L1 severe fractures after T12 and L2 conventional screw fixation and conventional screw

fixation during anterior flexion and posterior extension was respectively shown in Figs. 3 and 4.

Under the same fracture, the maximum von Mises stress of conventional pedicle screw (MC/UC) was larger than those of the Schanz pedicle screw (MS/US) ( $P < 0.05$ ). Under the same screws, the maximum von Mises stress of unstable fracture (UC/US) was larger than those of the moderate fracture (MC/MS) ( $P < 0.05$ ) (Tables 1 and 2).

### 10-Nm torque and 350-N vertical load during flexion, extension, lateral bending, and rotation

As shown in Fig. 5, the maximum von Mises stress of screws under a vertical load of 350 N and 10-Nm torque in each group was the largest in anterior flexion, followed by rotation, lateral bending, and posterior extension. The maximum von Mises stress of the upper screws during lateral bending, rotation, and posterior extension in each group was lower than the fatigue threshold. The maximum von Mises stress of the lower screws during flexion/extension, lateral bending, and rotation in each group was lower than the fatigue threshold. The maximum von Mises stress of the lower screws was lower than those of the upper screws during flexion, lateral bending, and rotation, and however it was larger than those of the upper screw during posterior extension.

Under the same fracture, the maximum von Mises stress of conventional pedicle screw (MC/UC) during lateral bending and rotation was larger than that of the Schanz screw (MS/US) ( $P < 0.05$ ). Under the same screw, the maximum von Mises stress of the upper screw of the unstable fracture during lateral bending and rotation was larger than that of the moderate fracture ( $P < 0.05$ ).

Under the same fracture, the maximum von Mises stress of the upper Schanz screw (MS/US) during posterior extension was larger than that of the upper conventional screw (MC/UC) ( $P < 0.05$ ). The maximum von Mises stress of UC during posterior extension was larger than that of MC ( $P < 0.05$ ). However, there was no significant difference regarding the maximum von Mises stress during posterior extension between US and MS ( $P > 0.05$ ).

### Postoperative axial displacement/micro-motion of the bony defect in lumbar 1

The maximum axial displacement/micro-motion (absolute value) of the bony defect in the vertebral body of lumbar 1 during flexion/extension, lateral bending, and rotation was located in the anterior margin of the upper vertebral body above the bony defect.

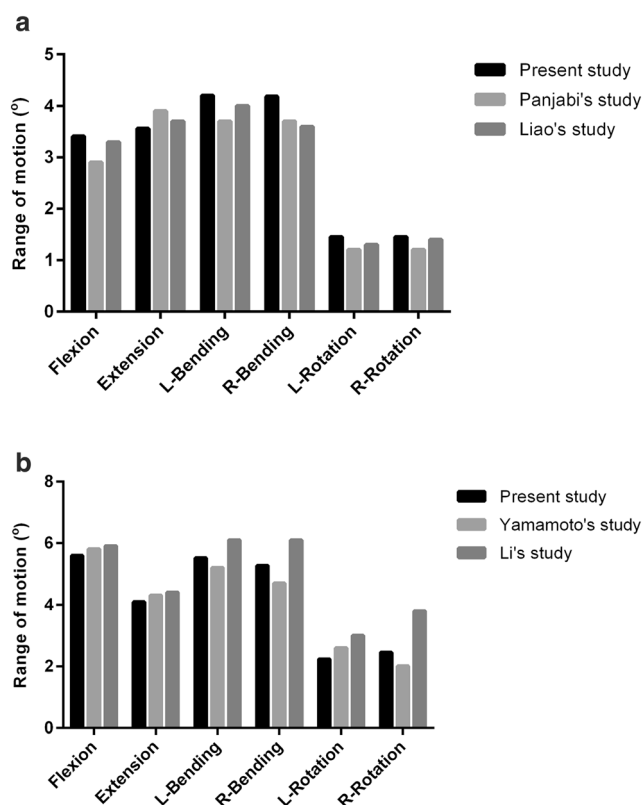


**Fig. 2** Comparison of range of motion (ROM) of T12/L1 and L1/L2 vertebrae of the normal T12-L2 model with other studies. **a** T12-L1 segment activity. **b** L1-L2 segment activity



**Table 1** Maximum stress of the upper screw (MPa) when torque, vertical load, and torque plus vertical load were applied

	MC	MS	UC	US
Torque				
5 Nm	96.0 ± 6.5* <sup>#</sup>	72.6 ± 7.4 <sup>#</sup>	165.8 ± 11.2*	122.8 ± 9.7
10 Nm	191.9 ± 13.0* <sup>#</sup>	145.2 ± 14.7 <sup>#</sup>	331.7 ± 22.4*	245.7 ± 19.4
15 Nm	287.9 ± 19.5* <sup>#</sup>	217.9 ± 22.1 <sup>#</sup>	497.5 ± 33.7*	368.5 ± 29.1
Vertical load				
150 N	96.1 ± 7.3* <sup>#</sup>	72.0 ± 6.4 <sup>#</sup>	166.0 ± 10.8*	126.3 ± 11.2
350 N	224.3 ± 17.0* <sup>#</sup>	168.0 ± 14.8 <sup>#</sup>	387.3 ± 25.1*	294.6 ± 26.1
500 N	320.4 ± 24.3* <sup>#</sup>	240.0 ± 21.2 <sup>#</sup>	553.3 ± 35.9*	420.9 ± 37.4
Torque plus vertical load				
350 N + 10 Nm	414.2 ± 28.6* <sup>#</sup>	306.0 ± 30.2 <sup>#</sup>	717.9 ± 42.8*	535.9 ± 42.9

\*MC vs MS group, or UC vs US group ( $P < 0.05$ )<sup>#</sup>MC vs UC group, or MS vs US group ( $P < 0.05$ )

### Pure torque or torque plus different vertical loads during anterior flexion

There was a “cohesive” displacement/micro-motion between UB and lower vertebral body (LB) (namely, downward displacement/micro-motion of UB and upward displacement/micro-motion of LB) in the bony defect of the lumbar 1 during anterior flexion. Furthermore, this displacement/micro-motion increased with the increase of the torque and/or load. Axial (Z-axis) displacement nephogram of the micro-motion of vertebral defect area at T12 and L2 conventional screw fixation and conventional screw fixation for L1 severe fracture during anterior flexion and posterior extension were shown in Figs. 6 and 7.

Under the same fracture, the axial displacement/micro-motion of UB above the bony defect in the MS/US group was larger than that in the MC/UC group ( $P < 0.05$ ) when pure torque was applied. When 10-Nm torque plus vertical load of 350 N or 500 N was applied, the axial displacement/micro-motion of UB of the bony defect in the MS/US group was larger than that in the MC/UC group ( $P < 0.05$ ) (Tables 3 and 4).

Under the same screws, the axial displacement/micro-motion of UB above the bony defect of L1 vertebral body in the UC/US group (unstable/severe fracture group) was larger than that in the MC/MS group (moderate fracture group) ( $P < 0.05$ ). The axial displacement/micro-motion of LB below the bony defect of L1 vertebra was similar to those of UB of the bony defect in each group (Tables 3 and 4).

### Displacement/micro-motion of L1 vertebra during flexion and extension, lateral bending, and rotation when 10-Nm torque plus a vertical load of 350 N was applied

The maximum axial displacement/micro-motion of UB above the bony defect of L1 vertebra under a vertical load of 350 N and 10-Nm torque in each group was the largest in anterior flexion, followed by lateral bending, rotation, and finally extension (Fig. 8).

Under the same fracture, the maximum axial displacement/micro-motion of the L1 vertebra of MS/US group was larger than that of MC/UC during lateral bending, rotation, and posterior extension ( $P < 0.05$ ). Under the same screws, the

**Table 2** Maximum stress (MPa) of the lower screw when torque, vertical load, and torque plus vertical load were applied

	MC	MS	UC	US
Torque				
5 Nm	66.1 ± 7.5* <sup>#</sup>	50.5 ± 6.1 <sup>#</sup>	116.7 ± 10.1*	86.3 ± 10.2
10Nm	132.3 ± 15.1* <sup>#</sup>	101.0 ± 12.1 <sup>#</sup>	233.4 ± 20.2*	172.6 ± 20.4
15 Nm	198.4 ± 22.6* <sup>#</sup>	151.4 ± 18.2 <sup>#</sup>	350.1 ± 30.2*	258.8 ± 30.5
Vertical load				
150 N	19.6 ± 9.5 <sup>#</sup>	17.8 ± 5.7 <sup>#</sup>	64.1 ± 20.2*	54.8 ± 15.3
350 N	45.8 ± 22.2 <sup>#</sup>	41.6 ± 13.3 <sup>#</sup>	149.6 ± 47.0*	127.8 ± 35.8
500 N	65.5 ± 31.7 <sup>#</sup>	59.4 ± 19.0 <sup>#</sup>	213.7 ± 67.2*	182.5 ± 51.1
Torque plus vertical load				
350 N + 10 Nm	162.3 ± 47.5* <sup>#</sup>	118.0 ± 38.1 <sup>#</sup>	381.3 ± 58.1*	291.3 ± 54.2

\*MC vs MS group, or UC vs US group ( $P < 0.05$ )<sup>#</sup>MC vs UC group, or MS vs US group ( $P < 0.05$ )

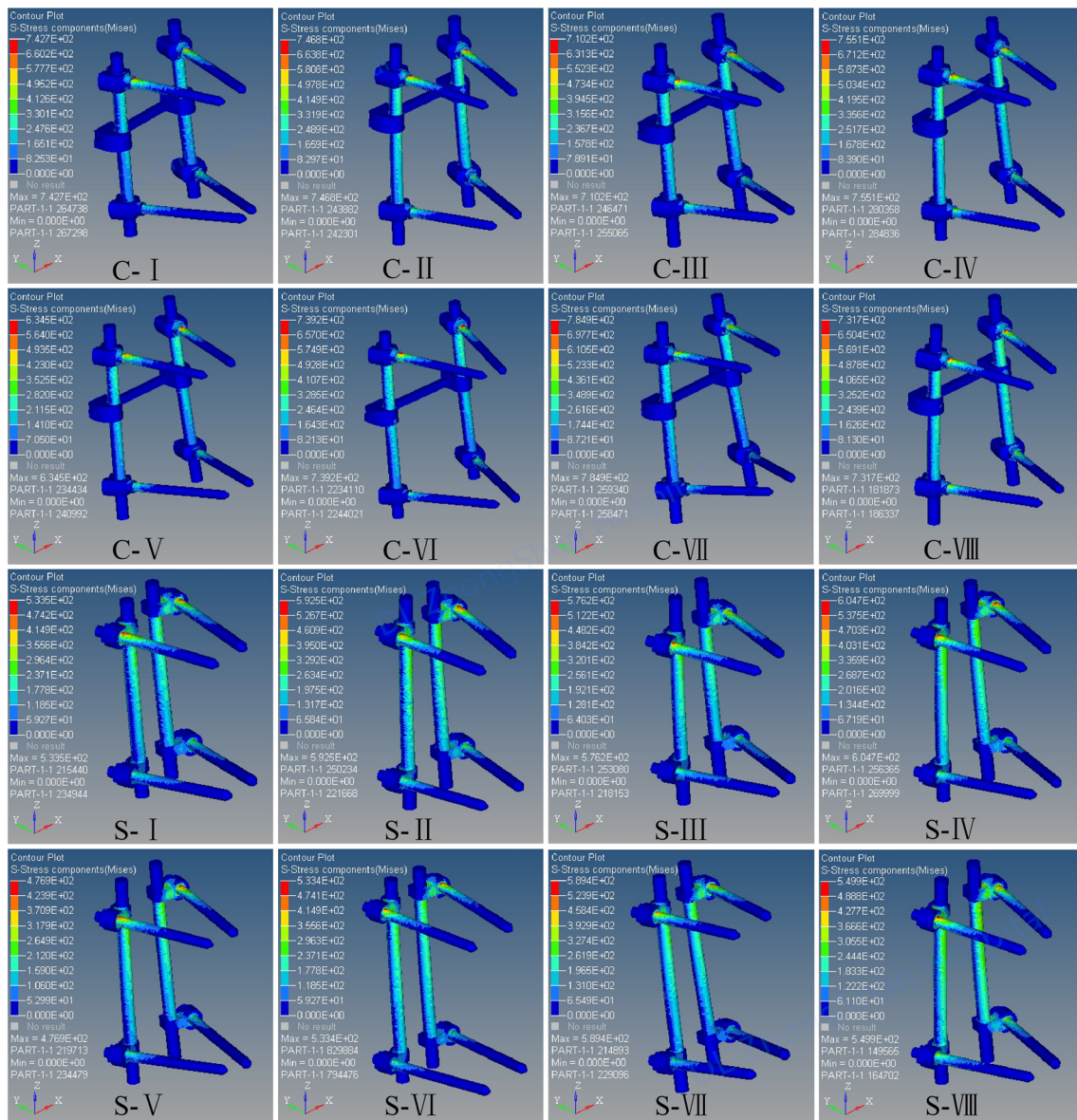


**Fig. 3** The stress nephogram of the L1 severe fractures after T12 and L2 pedicle screw fixation during anterior flexion. Red is the maximum stress. Eight models (I–VIII) of the conventional (C) pedicle screw group and the Schanz (S) pedicle screw group

maximum axial displacement/micro-motion of the injured L1 vertebrae in UC/US (severe fracture group) was significantly larger than that in the MC/MS group (moderate fracture group) ( $P < 0.05$ ) during lateral bending and rotation and was not significantly different during the extension ( $P > 0.05$ ).

## Discussion

Previous finite element studies of thoracolumbar fractures [13, 15, 16, 22] were mostly based on simulated analysis of one object, which was difficult to objectively evaluate the differences between conventional pedicle screws and Schanz pedicle screws. In this study, we collected 8 subjects for simulation in

order to avoid the deviation of the individual sample. For the 8 subjects, the size and curvature of vertebral bodies, the kyphotic angle of the T12-L2 segment, the actual screw length, and the actual height of the vertebral body were different. Therefore, the compression degree and screw depth of the models were analyzed by ratio and the reduction height of the injured vertebra was set to 100% to reduce the deviation. In addition, we evaluated the effects of different torques (5 Nm, 10 Nm, and 15 Nm) [19] and loads (150 N [22], 350 N [14], and 500 N [19]) on the stress of screws to explore the change tendency of screw stress with different loads and torques. Finally, 10 Nm and 350 N were selected as the main observation indexes.

Similar to the previous studies [12, 13], the maximum von Mises stress of pedicle screws in each group in this

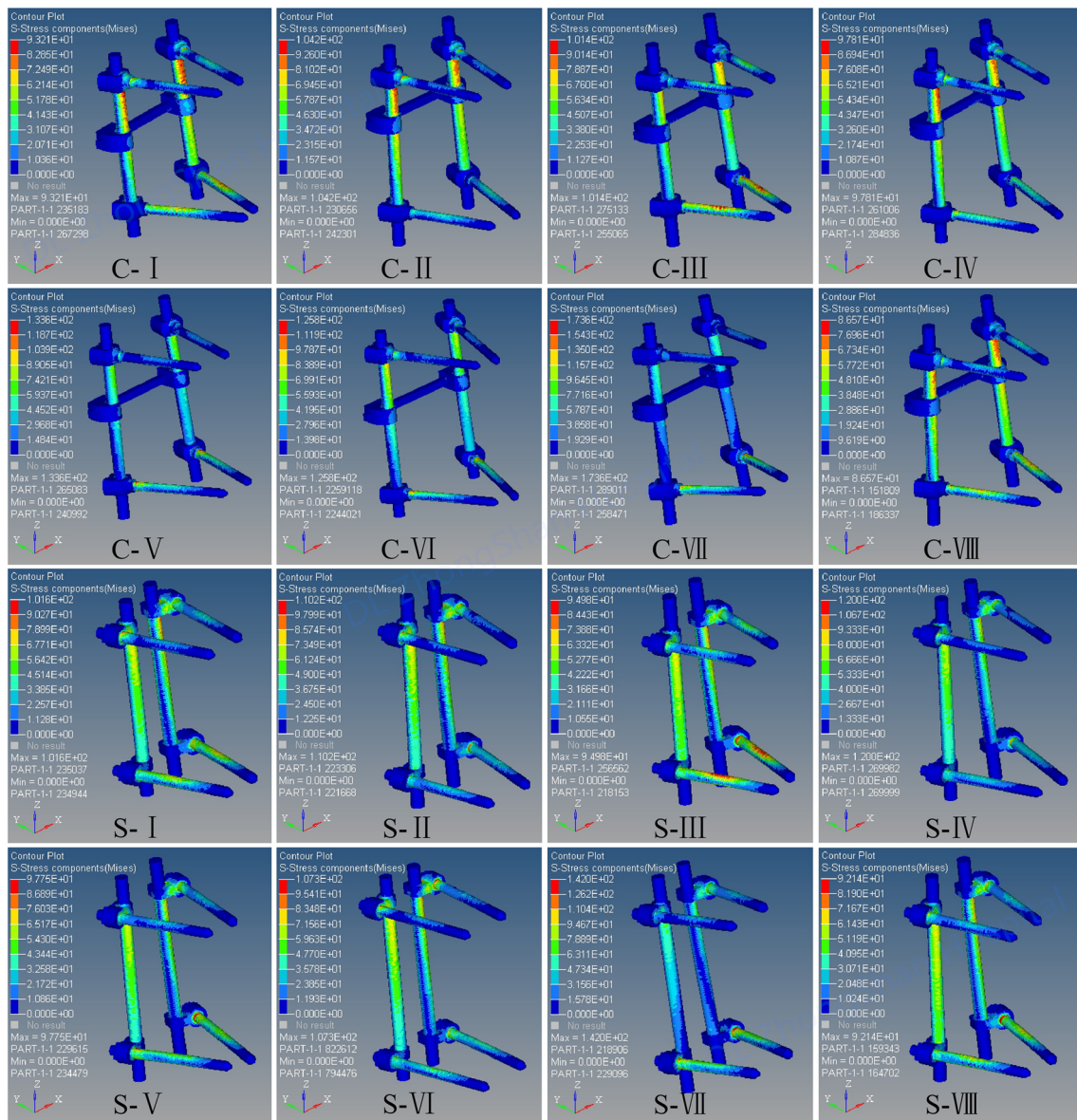


**Fig. 4** The stress nephogram of the L1 severe fractures after T12 and L2 pedicle screw fixation during posterior extension. Red is the maximum stress. Eight models (I–VIII) of the conventional (C) pedicle screw group and the Schanz (S) pedicle screw group

study occurred at the root of the upper screw and increased with the increase of torque and/or load. Additionally, the maximum von Mises stress of conventional pedicle screw was larger than that of the Schanz screw under the same fracture ( $P < 0.05$ ). The maximum von Mises stress of the upper screw of the unstable fracture was larger than that of the moderate fracture under the same screws ( $P < 0.05$ ). The maximum von Mises stress of the UC group was lower than the fatigue threshold of 550 MPa when pure vertical load of 550 N was applied and the stress of the other groups was lower, showing that both conventional and Schanz pedicle screws had a lower risk of screw breakage in an upright posture. Similarly, the findings indicated that these two

kinds of screws have a lower risk of screw breakage during extension, left and right bending, and rotation at the load of 350 N and torque of 10 Nm.

Anterior flexion is the most common and important way of spinal daily activity, which has the greatest impact on the pressure of the spine [19]. The results of this study showed that the stress of screws increased with the increase of the load when torque of 10 Nm was applied during flexion. We found that the screw stress of unstable fractures was larger than that of moderate fractures under the same screw, showing that the screws in unstable fractures bear more load than in moderate fractures, which was consistent with clinical practice. The stress of conventional pedicle screws was significantly higher than that of Schanz pedicle screws under the same fracture.



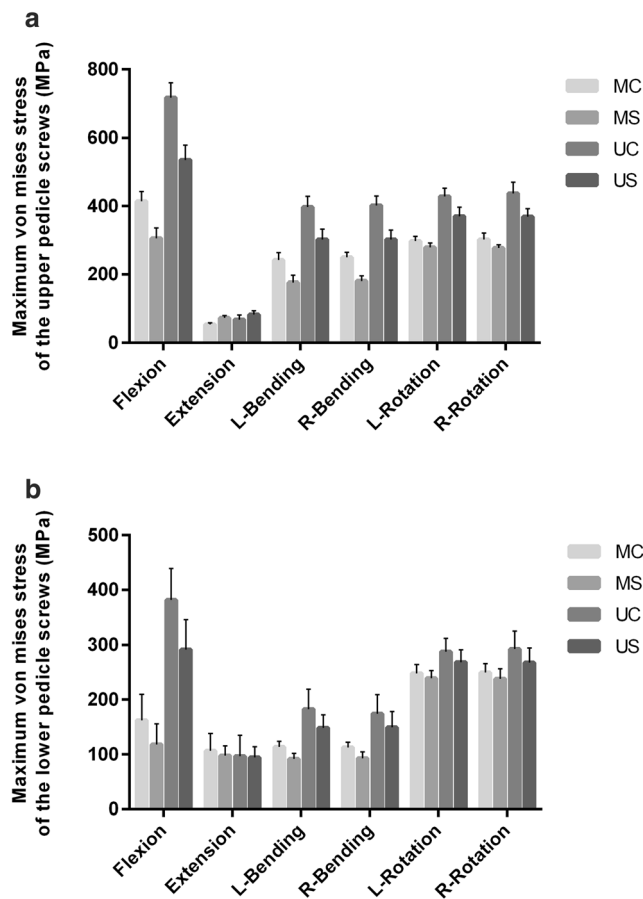


**Fig. 5** Simulation of maximum screw stress with 10-Nm torque plus a load of 350 N during flexion, extension, left and right bending, and left and right rotations. **a** Maximum von Mises stress of the upper screw in each group. The upper screw has the maximum von Mises stress during flexion, and the stress of UC group is higher than the fatigue threshold. **b** Maximum von Mises stress of the lower screw in each group. The maximum von Mises stress of the lower screw in each group is lower than the fatigue threshold

This may be due to the difference in structure and load transmission between the two screws because pedicle screw is to bear the load and conduct stress across the injured vertebra, and the latter capacity is more important than the former. Compared with the conventional pedicle screws, the Schanz pedicle screws can conduct the stress with less self-stress increase. In other words, the unloading capacity of Schanz pedicle screws is stronger than conventional pedicle screws.

The risk of screw breakage for moderate fractures is lower because the middle column of the injured vertebra remains partial load bearing and partial stress conduction; thus, the screw stress increase of moderate fractures was relatively insignificant. In view of the fact that conventional (percutaneous) pedicle screws have less damage to paravertebral soft tissue than Schanz screws, the former should be preferred in moderate fractures. For unstable fractures, the risk of screw breakage in the conventional screw (UC) group was greater than that in the Schanz screw (US)

group. This result is consistent with the author's previous hypothesis [10] and clinical practice. For type A severe fractures, the anterior and middle columns are unstable and cannot bear the load. All loads of the anterior, middle, and posterior columns had to transmit through the posterior screw rod. Unlike the normal lumbar posterior column (butterfly-shaped conduction), the structure and load transmission of conventional pedicle screw rod (similar to “|”-shaped conduction) may contribute to the significant stress increase and the instrumentation failure of conventional pedicle screw. Moreover, the augmentation of cement cannot avoid the breakage of pedicle screw either. Bu et al. [26, 27] indicated that screw breakage occurred in 2 of 28 cases after treatment with conventional pedicle screw instrumentation combined with vertebral cement injection. Elmasry et al. [27] used finite element analysis to evaluate the difference between percutaneous pedicle screw fixation (PPSF) and PPSF with injured vertebra balloon kyphoplasty (BKP), by creating two bone cement cavities symmetrically placed around the mid-sagittal plane, in the treatment of thoracolumbar burst fractures. They found that there was no significant difference in the percutaneous pedicle screw stress between these two methods, indicating that stress conduction is mainly transmitted through the screws and barely transmitted through bone cement in the injured vertebra. Furthermore, the stress of the pedicle screws in both methods during rotation and lateral bending was between 600 and 700 MPa, which is higher than the fatigue threshold of 529 MPa; they speculated that this overstress resulted in the long-term conventional pedicle screw fracture instrumentation failure after operation. The study [27] discussed above partially demonstrates our results and inferences that conventional pedicle screws are not suitable for unstable fractures.

Our results also indicated that flexion of the spine not only increases the stress of the pedicle screw but also has a significant effect on the bony defect displacement/micro-motion of the injured vertebra. This may be attributed to the upward displacement/micro-motion of LB below the bony defect caused by the reaction force of the rectus abdominis and the downward displacement/micro-motion of UB above the bony defect caused by the stress of load and the erector spinae during flexion [28]. To our best knowledge, we are the first to confirm that there is compression (cohesion) displacement/micro-motion in the bony defect area during anterior flexion, and we believe that this is the main cause of re-collapse of injured vertebrae with the increases of load/torque. We speculate that repeated displacement/micro-motion of this bone defect area not only limits the growth of new trabecular bone but also causes resorption of the grafted bone in the vertebral body. Subsequently, delayed union/non-union occurs and then results in the re-collapse of the injured vertebrae. In addition, the repeated displacement/micro-motion may also be the cause of non-union and ischemic necrosis of



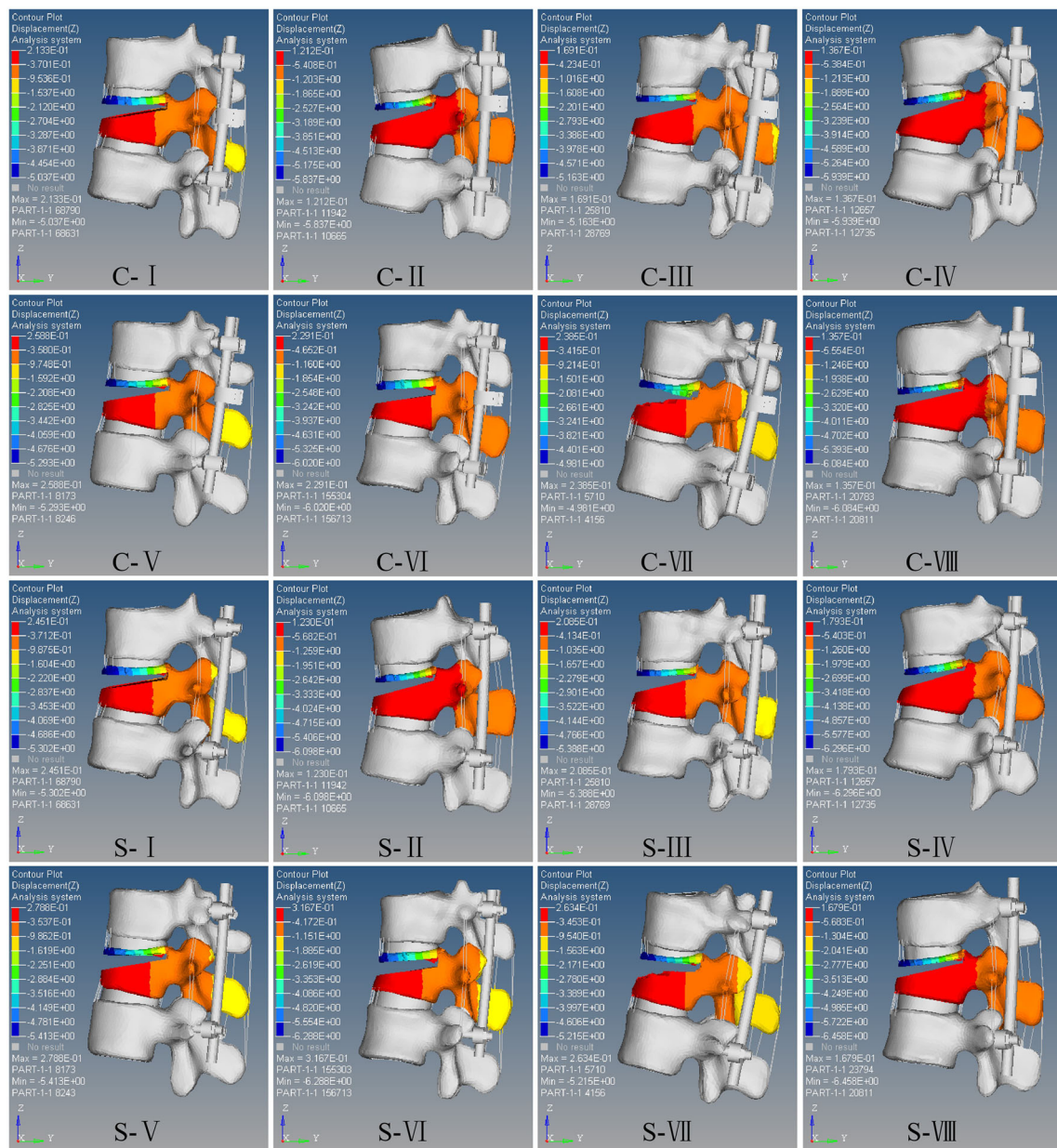


**Fig. 6** Axial (Z-axis) displacement nephogram of the micro-motion of vertebral defect area for L1 severe fracture with 10-Nm torque plus a load of 350 N during anterior flexion. Red is the maximum displacement

upward and blue is the maximum displacement downward. Eight models (I–VIII) of the conventional (C) pedicle screw group and the Schanz (S) pedicle screw group

osteoporotic vertebral fractures (Kummell disease); however, this remains to be confirmed. It is noteworthy that kyphosis recurrence and “cohesive” displacement/micro-motion of the bony defect occurred even when pure torque (simulate the lateral position) is applied.

The “cohesive” displacement/micro-motion of the bony defect of unstable fractures was larger than that of moderate fractures under the same screws ( $P < 0.05$ ). By retrospectively analyzing the re-collapse of thoracolumbar burst fractures after posterior pedicle screw instrumentation in 2018, Jang et al speculated that re-collapse was correlated with high reduction rate [11]. However, they have not proven this hypothesis. We,

in the present study, confirmed their hypothesis. Moreover, previous studies showed that re-collapse of injured vertebrae could not be avoided if unstable fractures were treated with solely Schanz pedicle screws or conventional pedicle screws [6, 29]. However, Schanz pedicle screws combined with TLSO treatment obtained good efficacy without re-collapse of injured vertebrae in our previous study [10]. Thus, for unstable fractures, we strongly advised that TLSO brace should be used to limit thoracolumbosacral activity during the early 3-month stage after operation to reduce the compression (cohesion) displacement/micro-motion of the bony defect in the vertebral body.

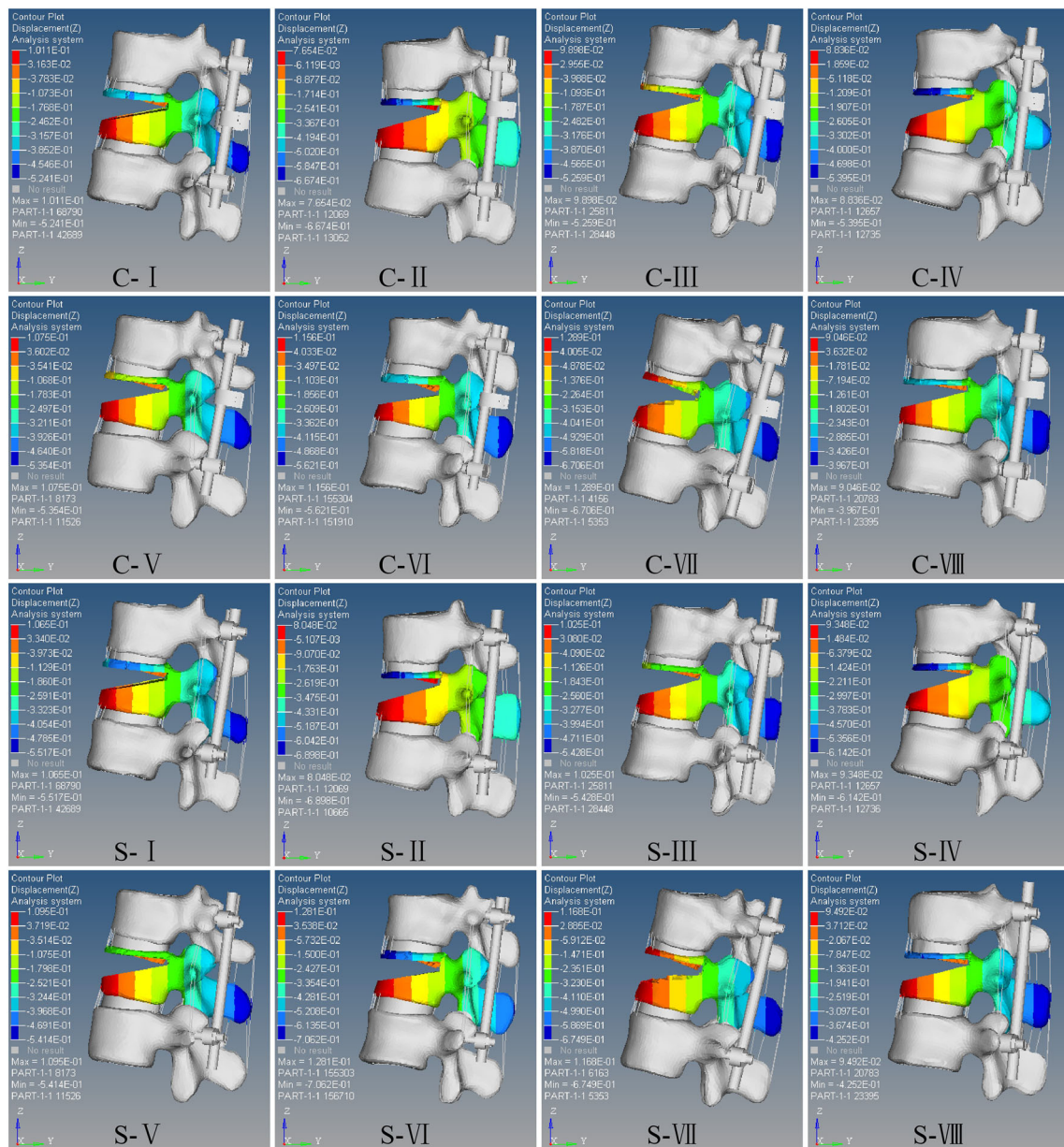


**Fig. 7** Axial (Z-axis) displacement nephogram of the micro-motion of vertebral defect area for L1 severe fracture with 10-Nm torque plus a load of 350 N during posterior extension. Red is the maximum displacement

upward and blue is the maximum displacement downward. Eight models (I–VIII) of the conventional (C) pedicle screw group and the Schanz (S) pedicle screw group

**Table 3** Maximum axial displacement (mm) of the upper vertebral body of bony defect during flexion when torque and torque plus vertical load were applied

	MC	MS	UC	US
Torque				
5 Nm	-0.69 ± 0.08* <sup>#</sup>	-0.69 ± 0.09 <sup>#</sup>	-1.32 ± 0.09*	-1.36 ± 0.09
10 Nm	-1.38 ± 0.16* <sup>#</sup>	-1.39 ± 0.17 <sup>#</sup>	-2.64 ± 0.17*	-2.72 ± 0.18
15 Nm	-2.07 ± 0.24* <sup>#</sup>	-2.08 ± 0.26 <sup>#</sup>	-3.96 ± 0.26*	-4.08 ± 0.26
Torque plus vertical load				
350 N + 10 Nm	-2.85 ± 0.39* <sup>#</sup>	-2.90 ± 0.41 <sup>#</sup>	-5.54 ± 0.47*	-5.81 ± 0.52

\*MC vs MS group, or UC vs US group ( $P < 0.05$ )

<sup>#</sup> MC vs UC group, or MS vs US group ( $P < 0.05$ )

**Table 4** Maximum axial displacement (mm) of the lower vertebral body of bony defect during flexion when torque and torque plus vertical load were applied

	MC	MS	UC	US
Torque				
5 Nm	0.00 ± 0.00 <sup>#</sup>	0.00 ± 0.00 <sup>#</sup>	0.02 ± 0.01*	0.03 ± 0.01
10 Nm	0.00 ± 0.00 <sup>#</sup>	0.00 ± 0.00 <sup>#</sup>	0.04 ± 0.02*	0.06 ± 0.03
15 Nm	0.00 ± 0.00 <sup>#</sup>	0.00 ± 0.00 <sup>#</sup>	0.07 ± 0.03*	0.09 ± 0.04
Torque plus vertical load				
350 N + 10 Nm	0.06 ± 0.04 <sup>*#</sup>	0.07 ± 0.03 <sup>#</sup>	0.19 ± 0.05*	0.22 ± 0.06

\*MC vs MS group, or UC vs US group ( $P < 0.05$ )

<sup>#</sup>MC vs UC group, or MS vs US group ( $P < 0.05$ )

One of the limitations of this study is that the results in our study were obtained by finite element analysis, which remains to be studied by further in vitro biomechanics experiments. Additionally, although the TLSO brace in our previous research [10] avoided the collapse of the injured vertebrae, whether TLSO brace has the function of preventing the vertebra from re-collapse should be verified by large randomized controlled study and related biomechanical experiments. Due to the presence of local curvature of the spine, the vertical load applied to simulate the gravity of the human body in the experiment is not a true vertical pressure. When applying pure compression load to the T12-L1 segment, there is a tendency of the local spine moving into flexion or extension that is why many authors proposed using a follower load. However, the stress of the normal spine is mainly transmitted through the anterior and middle columns when the follower load is applied, whereas the spine after fixation of the pedicle screw in our study is mainly transmitted through the posterior column (via the pedicle screw along the connecting rod which is

located in the posterior column) across the injured vertebrae. Although we collected 8 samples and applied multiple loads for comparative analysis, this simulation still needs to be improved, and a follower load suitable for the spine after pedicle screw fixation should be explored for correlation analysis in the future research.

For the moderate L1 fracture, short-segment instrumentation with conventional pedicle screw is preferred. However, Schanz pedicle screws were recommended for unstable fractures because the screws have a lower risk of screw breakage compared with conventional pedicle screws. The compression displacement/micro-motion of the bony defect of injured vertebrae during flexion may contribute to postoperative re-collapse of the injured vertebrae.

**Funding** This work was supported by the National Natural Science Foundation of China (grant 30870647) and Dalian Medical Scientific Research Project (grant 1811110).

## Compliance with ethical standards

**Conflict of interest** The authors declare that they have no competing interests.

**Ethical approval** This study was approved by the Ethics Committee of Affiliated Zhongshan Hospital of Dalian University.

**Informed consent** All participants provided written informed consent.

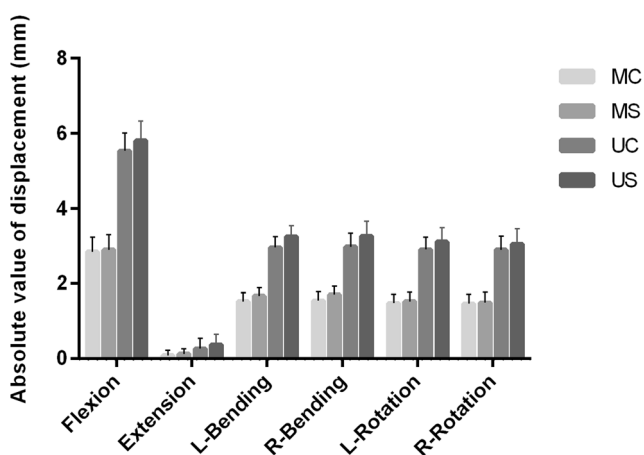


**Fig. 8** Simulation of the maximum axial displacement/micro-motion of L1 with 10-Nm torque plus a load of 350 N during flexion, extension, left and right bending, and left and right rotations. The maximum axial displacement/micro-motion with 10-Nm torque plus a load of 350 N in each group was the largest in anterior flexion, followed by lateral bending, rotation, and finally extension

## References

- Aono H, Tobimatsu H, Ariga K, Kuroda M, Nagamoto Y, Takenaka S, Furuya M, Iwasaki M (2016) Surgical outcomes of temporary short-segment instrumentation without augmentation for thoracolumbar burst fractures. *Injury* 47:1337–1344. <https://doi.org/10.1016/j.injury.2016.03.003>
- Mi J, Sun XJ, Zhang K, Zhao CQ, Zhao J (2018) Prediction of MRI findings including disc injury and posterior ligamentous complex injury in neurologically intact thoracolumbar burst fractures by the parameters of vertebral body damage on CT scan. *Injury* 49:272–278. <https://doi.org/10.1016/j.injury.2017.12.011>



3. Aono H, Ishii K, Tobimatsu H, Nagamoto Y, Takenaka S, Furuya M, Chiaki H, Iwasaki M (2017) Temporary short-segment pedicle screw fixation for thoracolumbar burst fractures: comparative study with or without vertebroplasty. *Spine J: Off J North Am Spine Soc* 17:1113–1119. doi:<https://doi.org/10.1016/j.spinee.2017.03.022>
4. Xu GJ, Li ZJ, Ma JX, Zhang T, Fu X, Ma XL (2013) Anterior versus posterior approach for treatment of thoracolumbar burst fractures: a meta-analysis. *Eur Spine J : Off Publ Eur Spine Soc, Eur Spinal Deform Soc Eur Sect Cervical Spine Res Soc* 22:2176–2183. <https://doi.org/10.1007/s00586-013-2987-y>
5. McCormack T, Karaikevic E, Gaines RW (1994) The load sharing classification of spine fractures. *Spine* 19:1741–1744
6. Pneumaticos SG, Triantafyllopoulos GK, Giannoudis PV (2013) Advances made in the treatment of thoracolumbar fractures: current trends and future directions. *Injury* 44:703–712. <https://doi.org/10.1016/j.injury.2012.12.005>
7. Ozdemir B, Kanat A, Erturk C, Batcik OE, Balik MS, Yazar U, Celiker FB, Metin Y, Inecikli MF, Guvercin AR (2017) Restoration of anterior vertebral height by short-segment pedicle screw fixation with screwing of fractured vertebra for the treatment of unstable thoracolumbar fractures. *World Neurosurg* 99:409–417. <https://doi.org/10.1016/j.wneu.2016.11.133>
8. Kanna RM, Shetty AP, Rajasekaran S (2015) Posterior fixation including the fractured vertebra for severe unstable thoracolumbar fractures. *Spine J: Off J N Am Spine Soc* 15:256–264. <https://doi.org/10.1016/j.spinee.2014.09.004>
9. Pellise F, Barastegui D, Hernandez-Fernandez A, Barrera-Ochoa S, Bago J, Issa-Benitez D, Caceres E, Villanueva C (2015) Viability and long-term survival of short-segment posterior fixation in thoracolumbar burst fractures. *Spine J: Off J N Am Spine Soc* 15:1796–1803. <https://doi.org/10.1016/j.spinee.2014.03.012>
10. Yang S, Shang DP, Lu JM, Liu JF, Fu DP, Zhou F, Cong Y, Lv ZZ (2018) Modified posterior short-segment pedicle screw instrumentation for lumbar burst fractures with incomplete neurological deficit. *World Neurosurg* 119:e977–e985. <https://doi.org/10.1016/j.wneu.2018.08.014>
11. Jang HD, Bang C, Lee JC, Soh JW, Choi SW, Cho HK, Shin BJ (2018) Risk factor analysis for predicting vertebral body re-collapse after posterior instrumented fusion in thoracolumbar burst fracture. *Spine J : Off J N Am Spine Soc* 18:285–293. doi:<https://doi.org/10.1016/j.spinee.2017.07.168>
12. Liu J, Yang S, Lu J, Fu D, Liu X, Shang D (2018) Biomechanical effects of USS fixation with different screw insertion depths on the vertebrae stiffness and screw stress for the treatment of the L1 fracture. *J Back Musculoskel Rehab* 31:285–297. <https://doi.org/10.3233/bmr-169692>
13. Xu G, Fu X, Du C, Ma J, Li Z, Tian P, Zhang T, Ma X (2014) Biomechanical comparison of mono-segment transpedicular fixation with short-segment fixation for treatment of thoracolumbar fractures: a finite element analysis. *Proc Inst Mech Eng H J Eng Med* 228:1005–1013. <https://doi.org/10.1177/0954411914552308>
14. Kubosch D, Kubosch EJ, Gueorguiev B, Zderic I, Windolf M, Izadpanah K, Sudkamp NP, Strohm PC (2016) Biomechanical investigation of a minimally invasive posterior spine stabilization system in comparison to the Universal Spinal System (USS). *BMC Musculoskelet Disord* 17:134. <https://doi.org/10.1186/s12891-016-0983-1>
15. Liao JC, Chen WP, Wang H (2017) Treatment of thoracolumbar burst fractures by short-segment pedicle screw fixation using a combination of two additional pedicle screws and vertebroplasty at the level of the fracture: a finite element analysis. *BMC Musculoskelet Disord* 18:262. <https://doi.org/10.1186/s12891-017-1623-0>
16. Alizadeh M, Kadir MR, Fadhli MM, Fallahiarezoodar A, Azmi B, Murali MR, Kamarul T (2013) The use of X-shaped cross-link in posterior spinal constructs improves stability in thoracolumbar burst fracture: a finite element analysis. *J Orthop Res : Off Publ Orthop Res Soc* 31:1447–1454. <https://doi.org/10.1002/jor.22376>
17. Chen SH, Chiang MC, Lin JF, Lin SC, Hung CH (2013) Biomechanical comparison of three stand-alone lumbar cages—a three-dimensional finite element analysis. *BMC Musculoskelet Disord* 14:281. <https://doi.org/10.1186/1471-2474-14-281>
18. Li C, Zhou Y, Wang H, Liu J, Xiang L (2014) Treatment of unstable thoracolumbar fractures through short segment pedicle screw fixation techniques using pedicle fixation at the level of the fracture: a finite element analysis. *PLoS One* 9:e99156. <https://doi.org/10.1371/journal.pone.0099156>
19. Naserkhaki S, El-Rich M (2017) Sensitivity of lumbar spine response to follower load and flexion moment: finite element study. *Computer methods in biomechanics and biomedical engineering* 20:550–557. <https://doi.org/10.1080/10255842.2016.1257707>
20. Rohlmann A, Neller S, Claes L, Bergmann G, Wilke HJ (2001) Influence of a follower load on intradiscal pressure and intersegmental rotation of the lumbar spine. *Spine* 26:E557–E561
21. Vaccaro AR, Oner C, Kepler CK, Dvorak M, Schnake K, Bellabarba C, Reinhold M, Aarabi B, Kandziora F, Chapman J, Shanmuganathan R, Fehlings M, Vialle L (2013) AOSpine thoracolumbar spine injury classification system: fracture description, neurological status, and key modifiers. *Spine* 38:2028–2037. <https://doi.org/10.1097/BRS.0b013e3182a8a381>
22. Wang H, Zhao Y, Mo Z, Han J, Chen Y, Yu H, Wang Q, Liu J, Li C, Zhou Y, Xiang L (2017) Comparison of short-segment monoaxial and polyaxial pedicle screw fixation combined with intermediate screws in traumatic thoracolumbar fractures: a finite element study and clinical radiographic review. *Clinics (Sao Paulo, Brazil)* 72:609–617. [https://doi.org/10.6061/clinics/2017\(10\)04](https://doi.org/10.6061/clinics/2017(10)04)
23. Panjabi MM, Oxland TR, Lin RM, McGowen TW (1994) Thoracolumbar burst fracture. A biomechanical investigation of its multidirectional flexibility. *Spine* 19:578–585
24. Yamamoto I, Panjabi MM, Crisco T, Oxland T (1989) Three-dimensional movements of the whole lumbar spine and lumbosacral joint. *Spine* 14:1256–1260
25. Brown SA (2006) Chapter 2—synthetic biomaterials for spinal applications. *Spine Technology Handbook*:11–33
26. Bu BX, Wang MJ, Liu WF, Wang YS, Tan HL (2015) Short-segment posterior instrumentation combined with calcium sulfate cement vertebroplasty for thoracolumbar compression fractures: radiographic outcomes including nonunion and other complications. *Orthopaedics & traumatology, surgery & research : OTSR* 101:227–233. <https://doi.org/10.1016/j.otsr.2014.11.019>
27. Elmasry SS, Asfour SS, Travascio F (2018) Finite element study to evaluate the biomechanical performance of the spine after augmenting percutaneous pedicle screw fixation with kyphoplasty in the treatment of burst fractures. *J Biomech Eng* 140:061005. <https://doi.org/10.1115/1.4039174>
28. Wilke HJ, Rohlmann A, Neller S, Graichen F, Claes L, Bergmann G (2003) ISSLS prize winner: a novel approach to determine trunk muscle forces during flexion and extension: a comparison of data from an in vitro experiment and in vivo measurements. *Spine* 28:2585–2593. <https://doi.org/10.1097/01.brs.0000096673.16363.c7>
29. Lakshmanan P, Jones A, Mehta J, Ahuja S, Davies PR, Howes JP (2009) Recurrence of kyphosis and its functional implications after surgical stabilization of dorsolumbar unstable burst fractures. *Spine J : Off J N Am Spine Soc* 9:1003–1009. doi:<https://doi.org/10.1016/j.spinee.2009.08.457>

**Publisher's note** Springer Nature remains neutral with regard to jurisdictional claims in published maps and institutional affiliations.